Antileishmanial activity of sp^2-iminosugar derivatives

Elena M. Sánchez-Fernández,[a,1] Verónica Gómez-Pérez,[b,1] Raquel García-Hernández,[b] José Manuel García Fernández,[c] Gabriela B. Plata,[d] José M. Padrón,[d] Carmen Ortiz Mellet,*[a,2] Santiago Castanys,*[b,2] Francisco Gamarro*[b,2]

[a] Departamento de Química Orgánica, Facultad de Química, Universidad de Sevilla, Apartado 553, E-41071, Spain.

[b] Instituto de Parasitología y Biomedicina "López-Neyra", IPBLN-CSIC, Parque Tecnológico de Ciencias de la Salud, 18016-Granada, Spain.

[c] Instituto de Investigaciones Químicas (IIQ), CSIC - Universidad de Sevilla, Avda. Américo Vespucio 49, 41092, Sevilla, Spain.

[d] BioLab, Instituto Universitario de Bio-Orgánica "Antonio González", Centro de Investigaciones Biomédicas de Canarias, Universidad de La Laguna, 38206, La Laguna, Spain..

[1] Both authors contributed equally to this manuscript

[2] Equal senior investigators in this study

List of Contents

1. General Procedure for the Glycosidase Inhibition Assay

Inhibitory potencies were determined by spectrophotometrically measuring the residual hydrolytic activities of the glycosidases against the respective *o*- (for β-glucosidase/β-galactosidase from bovine liver and β-galactosidase from *E. coli*) or *p*-nitrophenyl α- or β-D-glycopyranoside, in the presence of the corresponding inhibitor. Each assay was performed in phosphate buffer at the optimal pH for each enzyme. The K_m values for the different glycosidases used in the tests and the corresponding working pHs are listed herein: α-glucosidase (yeast), K_m = 0.35 mM (pH 6.8); isomaltase (yeast) K_m = 1.0 mM (pH 6.8), β-glucosidase (almonds), K_m = 3.5 mM (pH 7.3); β-glucosidase/β-galactosidase (bovine liver), K_m = 2.0 mM (pH 7.3); β- galactosidase (*E. coli*), K_m = 0.12 mM (pH 7.3); α-galactosidase (coffee beans), K_m = 2.0 mM (pH 6.8); trehalase (pig kidney), K_m = 4.0 mM (pH 6.2); amyloglucosidase (*Aspergillus niger*), K_m = 3.0 mM (pH 5.5); β-mannosidase (*Helix pomatia*), K_m = 0.6 mM (pH 5.5); α-mannosidase (jack bean), K_m = 2.0 mM (pH 5.5); naringinase (*Penicillium decumbens*, β-glucosidase/β-rhamnosidase activity). The reactions were initiated by addition of enzyme to a solution of the substrate in the absence or presence of various concentrations of inhibitor. After the mixture was incubated for 10-30 min at 37 ºC or 55 ºC the reaction was quenched by addition of 1 M Na_2CO_3. The absorbance of the resulting mixture was determined at 405 nm or 505 nm. Each experiment was performed in duplicate using [I] = 2, 0.4, 0.08, 0.04 y 0.02 μM and [S] nearly K_m value. In those cases were K_i values lower that 10 μM were obtained by this procedure (**2α, 5, 7** and **8** against yeast α-glucosidase), refined K_i values and the enzyme inhibition mode were determined from the slope of Lineweaver-Burk plots and double reciprocal analysis (Figures S1-S4).

2. Lineweaver-Burk and Double Reciprocal Analysis Plots

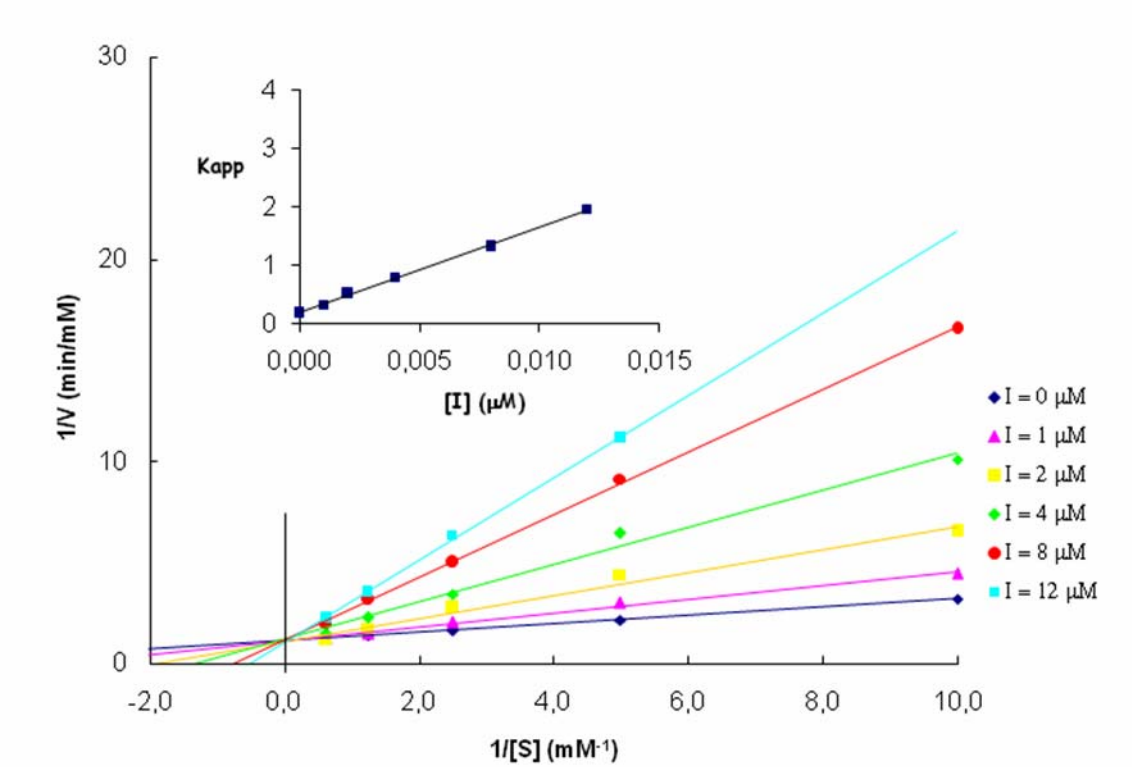

Figure S1. Lineweaver-Burk Plot for K_i determination (1.3 µM) of **2α** against α-glucosidase (baker yeast) (pH 6.8).

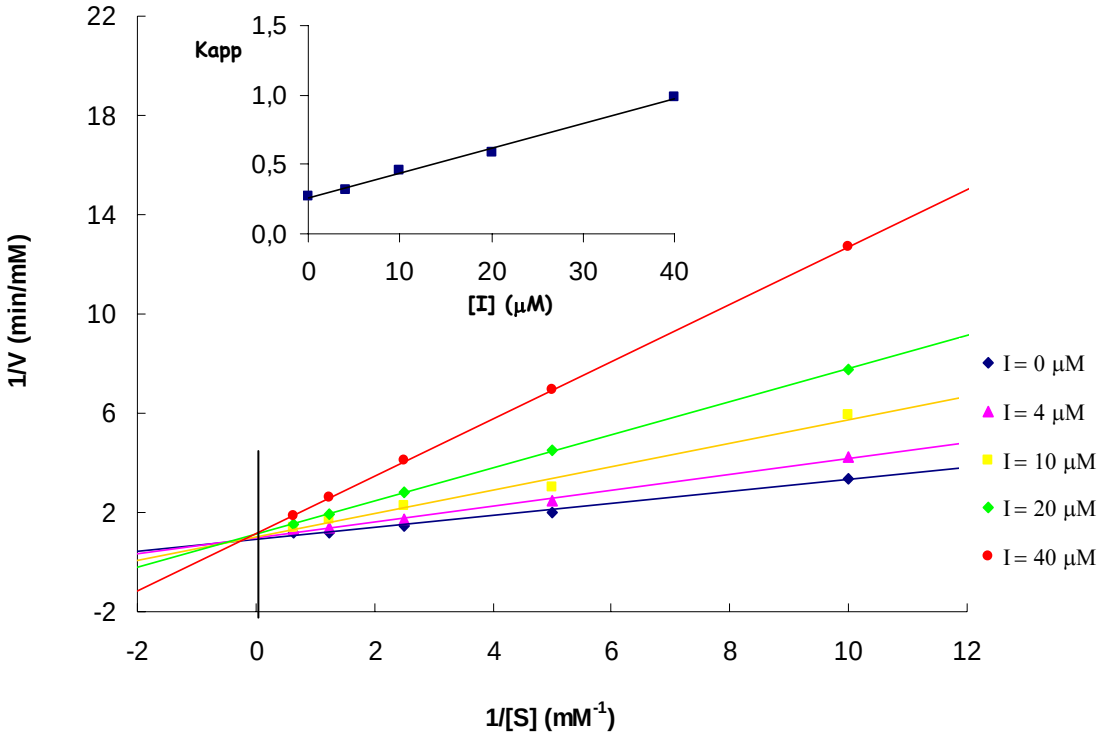

Figure S2. Lineweaver-Burk Plot for K_i determination (14.3 µM) of **5** against α-glucosidase (baker yeast) (pH 6.8).

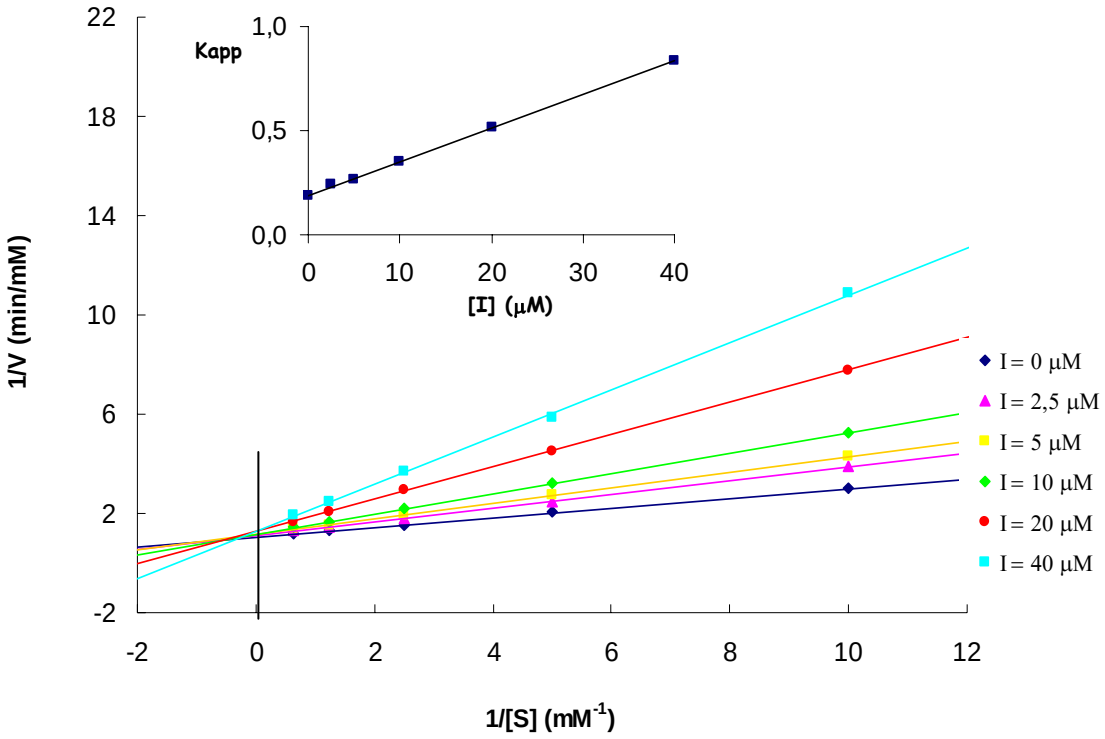

Figure S3. Lineweaver-Burk Plot for K_i determination (11.8 µM) of **7** against α-glucosidase (baker yeast) (pH 6.8).

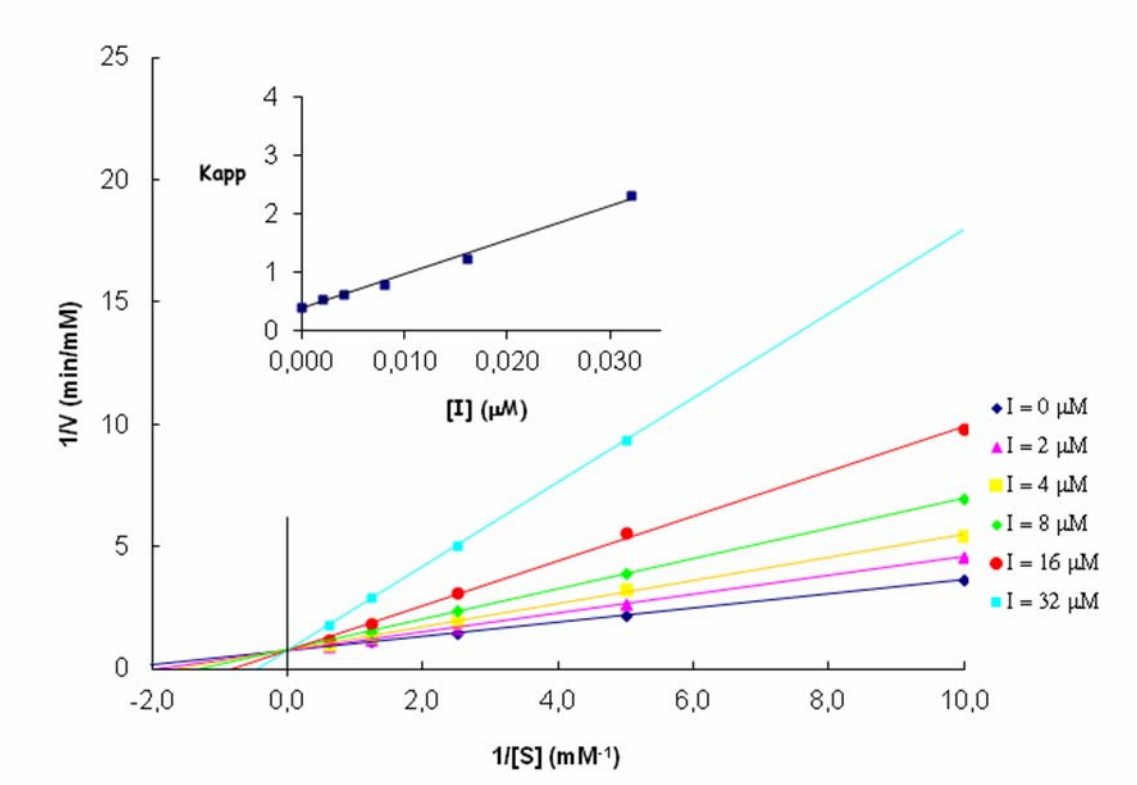

Figure S4. Lineweaver-Burk Plot for K_i determination (6.4 µM) of **8** against α-glucosidase (baker yeast) (pH 6.8).

3. Spectroscopic Data of 13β and 2β

(1*S*)-2,3,4-Tri-*O*-acetyl-1-dodecylthio-5*N*,6*O*-oxomethylidenenojirimycin (13β): Column chromatography (1:5 → 1:2 EtOAc:cyclohexane). Yield: 33 mg (6%). White solid. R_f 0.67 (1:1 EtOAc-cyclohexane). $[\alpha]_D$ +4.9 (*c* 1.0 in DCM). ^{1}H NMR (500 MHz, $CDCl_3$) δ 5.19 (dd, 1 H, $J_{4,5}$ = 10.5 Hz, $J_{3,4}$ = 7.0 Hz, H-4), 5.13 (t, 1 H, $J_{1,2} = J_{2,3}$ = 4.0 Hz, H-2), 5.02 (dd, 1 H, H-3), 4.62 (d, 1 H, H-1), 4.33 (dd, 1 H, $J_{6a,6b}$ = 8.8 Hz, $J_{5,6a}$ = 7.7 Hz, H-6a), 4.08 (t, 1 H, $J_{5,6b}$ = 8.8 Hz, H-6b), 3.90 (ddd, 1 H, H-5), 2.87-2.74 (m, 2 H, SCH_2), 2.08-1.98 (3 s, 9 H, MeCO), 1.65-1.10 (m, 20 H, CH_2), 0.81 (t, 3 H, $^3J_{H,H}$ = 7.0 Hz, CH_3). ^{13}C NMR (125.7 MHz, $CDCl_3$) δ 169.8-168.7 (Me*CO*), 156.0 (CO), 73.6 (C-3), 73.3 (C-2), 72.7 (C-4), 67.1 (C-6), 59.2 (C-1), 53.9 (C-5), 34.3 (SCH_2), 31.9-22.7 (CH_2), 20.8-20.6 (*Me*CO), 14.1 (CH_3). ESIMS: *m/z* 538.4 $[M + Na]^+$. Anal. Calcd for $C_{25}H_{41}NO_8S$: C 58.23, H 8.01, N 2.72, S 6.22. Found: C 57.86, H 7.73, N 2.63, S 6.47.

(1*S*)-1-Dodecylthio-5*N*,6*O*-oxomethylidenenojirimycin (2β): Yield: 18 mg (91%). R_f 0.80 (1:5 MeOH-EtOAc). $[\alpha]_D$ -9.0 (*c* 1.3 in DMSO). ^{1}H NMR (400 MHz, DMSO-d_6) δ 4.29 (dd, 1 H, $J_{6a,6b}$ = 8.6 Hz, $J_{5,6a}$ = 7.0 Hz, H-6a), 4.21 (d, 1 H, $J_{1,2}$ = 8.0 Hz, H-1), 4.05 (dd, 1 H, $J_{5,6b}$ = 4.6 Hz, H-6b), 3.60 (dd, 1 H, $J_{4,5}$ = 10.0 Hz, H-5), 2.73-2.62 (m, 2 H, SCH_2), 1.52 (quint., 1 H, $^3J_{H,H}$ = 7.0 Hz, SCH_2CH_2), 1.40-1.20 (m, 18 H, CH_2), 0.86 (t, 3 H, $^3J_{H,H}$ = 7.0 Hz, CH_3). ^{13}C NMR (75.5 MHz, DMSO-d_6) δ 156.0 (CO), 77.6-72.6 (C-3, C-4), 74.7 (C-2), 65.8 (C-6), 62.5 (C-1), 57.9 (C-5), 33.3 (SCH_2), 31.3-22.2 (CH_2), 14.0 (CH_3). ESIMS: *m/z* 412.3 $[M + Na]^+$. Anal. Calcd for $C_{19}H_{35}NO_5S$: C 58.58, H 9.06, N 3.60, S 8.23. Found: C 58.32, H 8.88, N 3.39, S 7.85.

4. Copies of ^{1}H and ^{13}C NMR Spectra

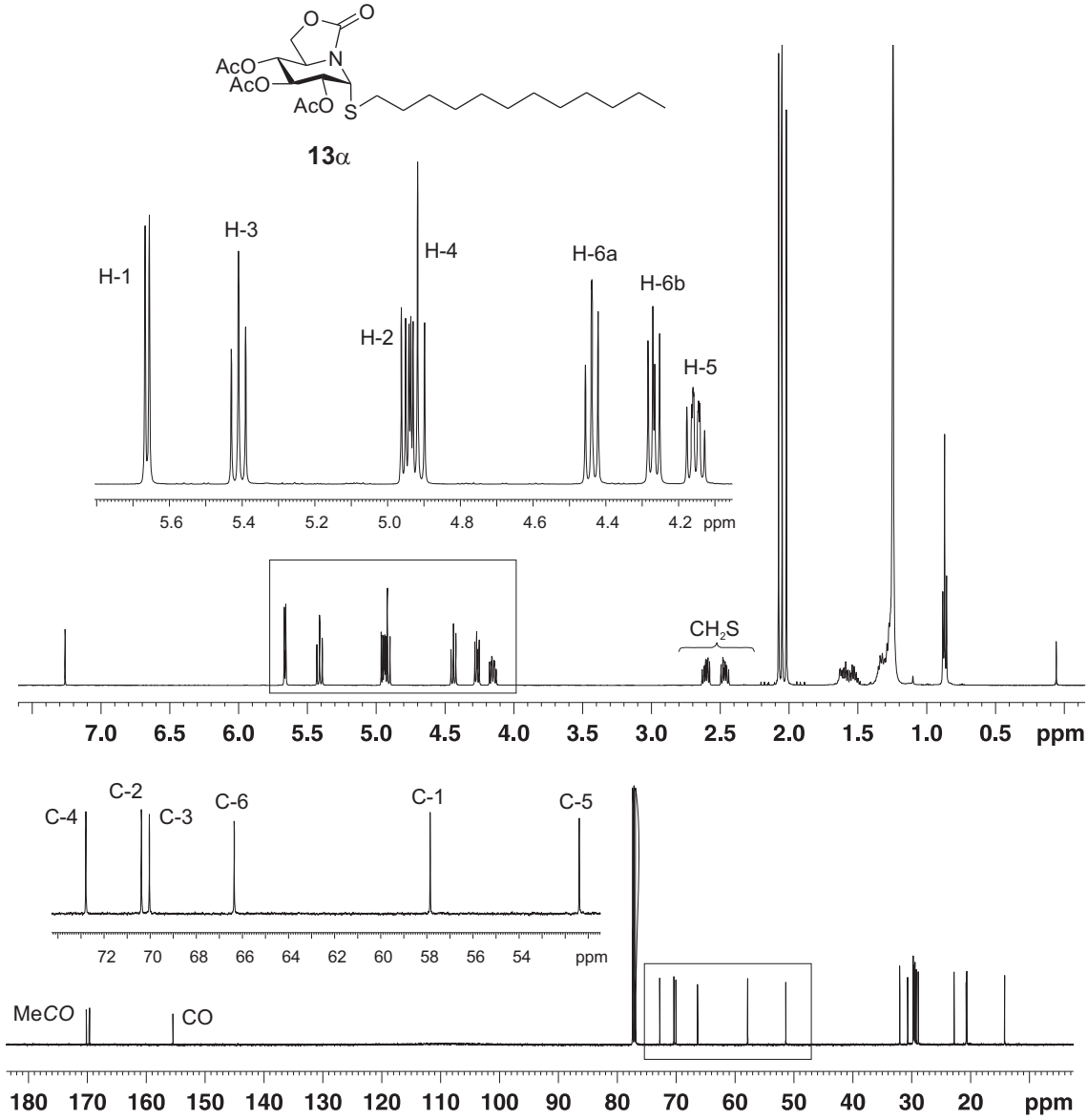

Figure S5. ^{1}H and ^{13}C NMR spectra (500 MHz and 125.7 MHz, $CDCl_3$) of **13α**

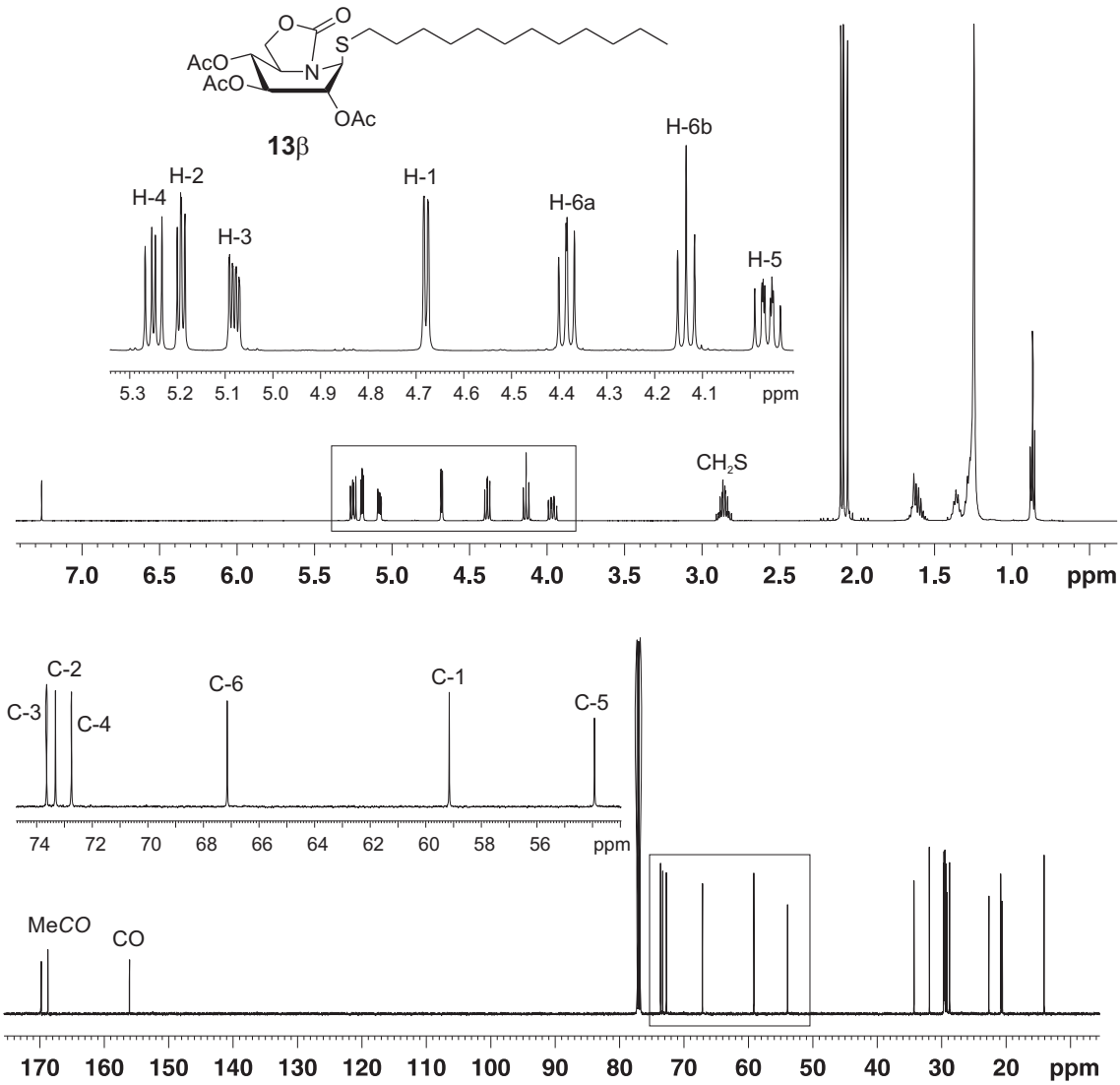

Figure S6. ^{1}H and ^{13}C NMR spectra (500 MHz and 125.7 MHz, $CDCl_3$) of **13β**

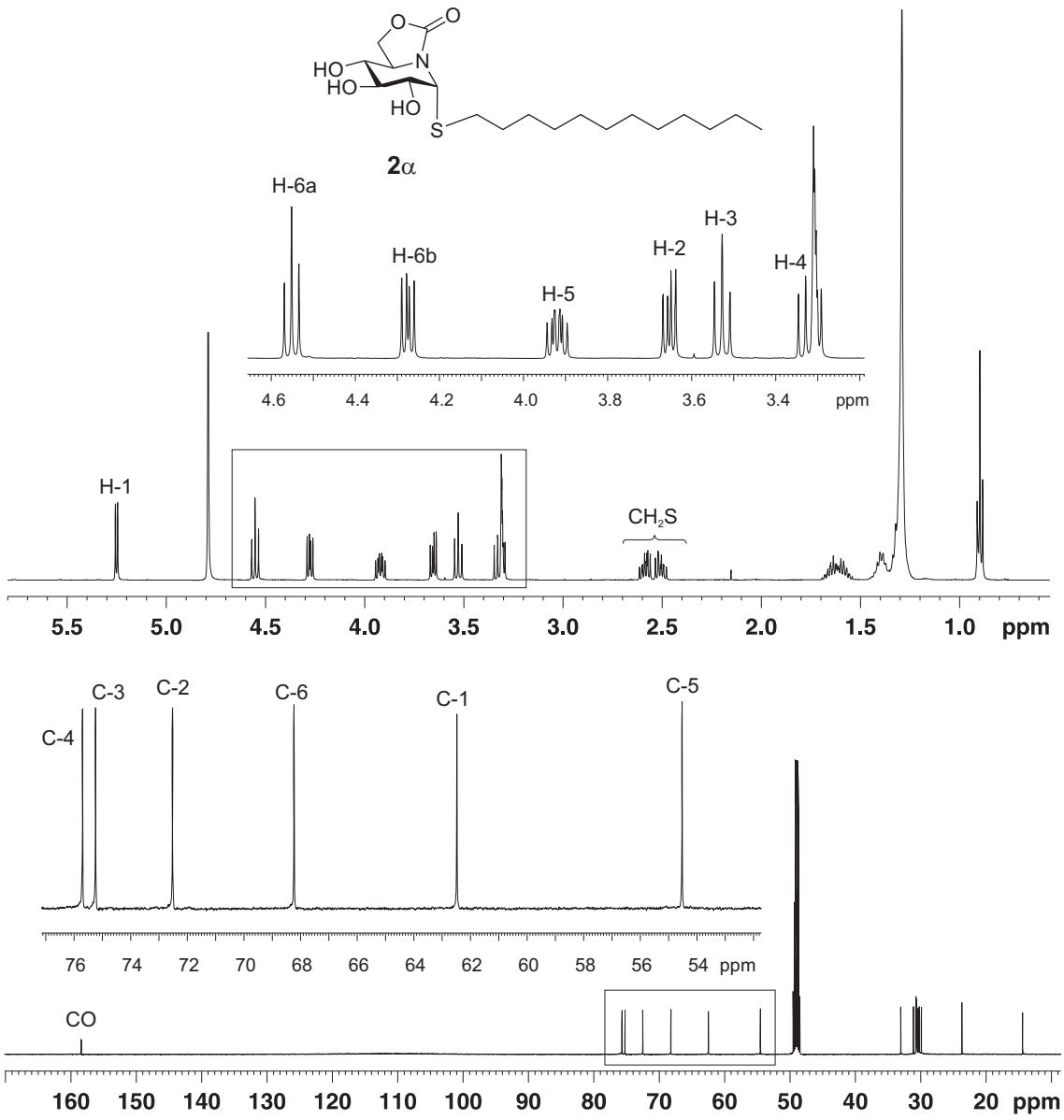

Figure S7. ^{1}H and ^{13}C NMR spectra (500 MHz and 125.7 MHz, CD_3OD) of **2α**

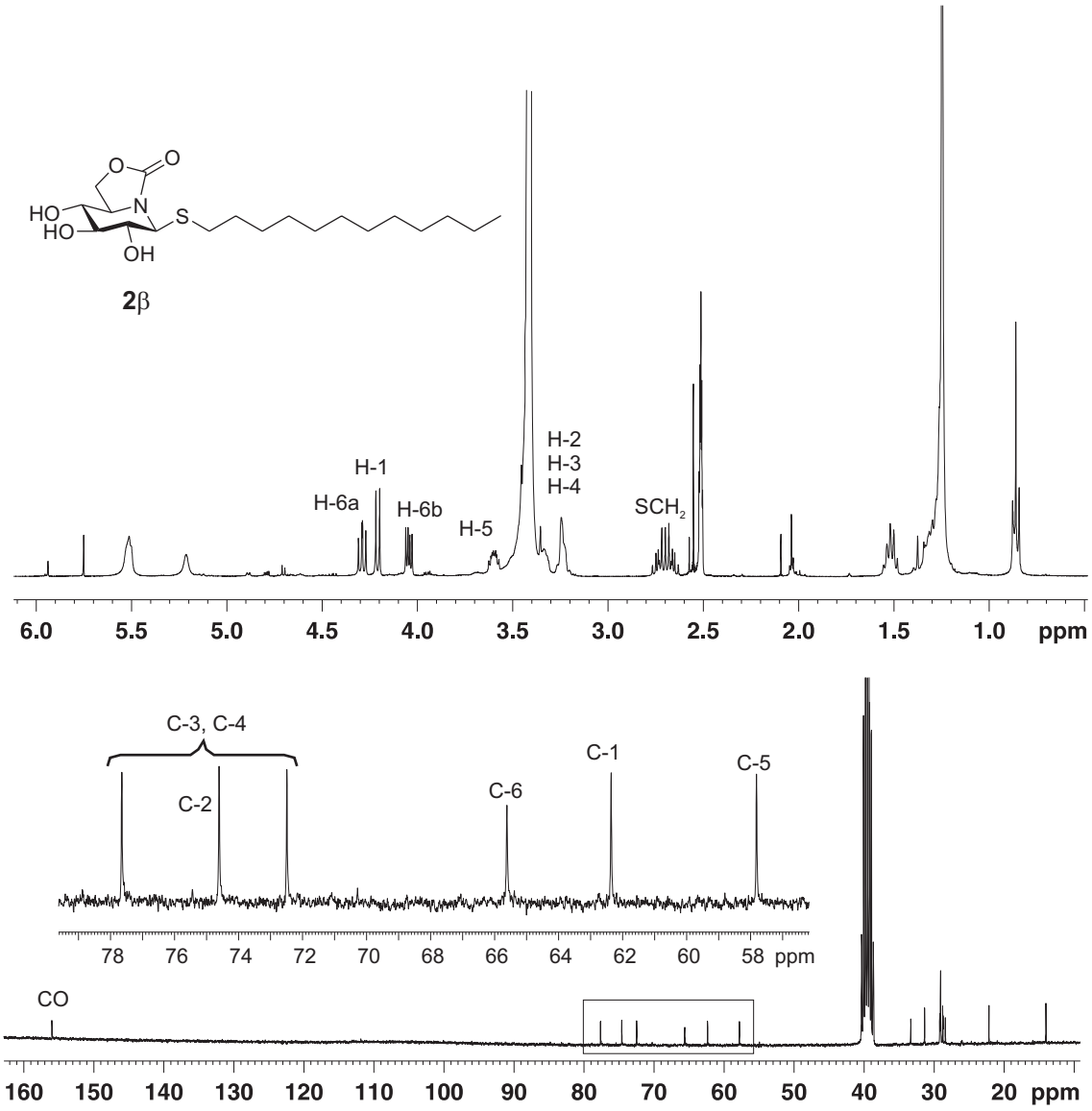

Figure S8. ^{1}H and ^{13}C NMR spectra (400 MHz and 75.5 MHz, DMSO-d_6) of **2β**

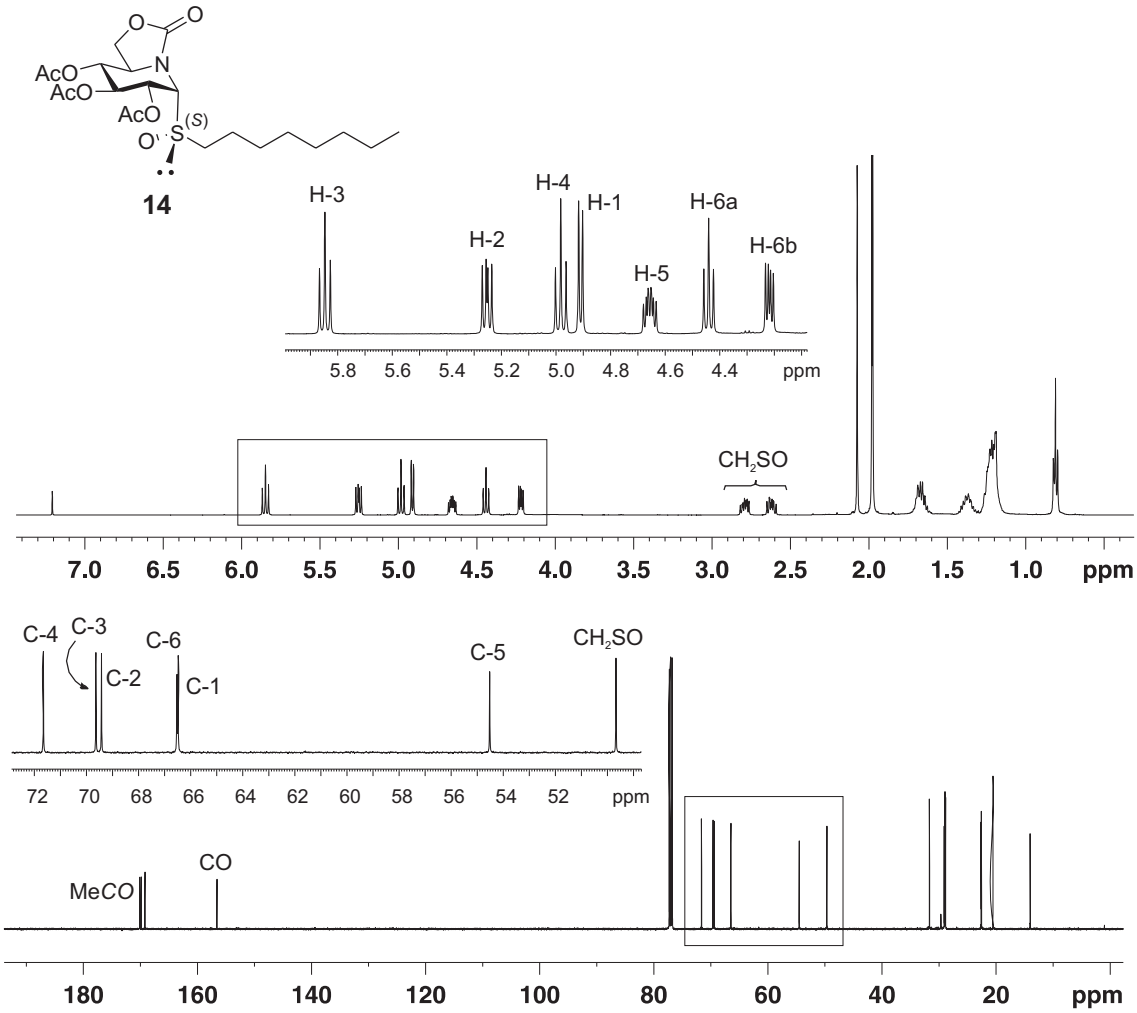

Figure S9. ^{1}H and ^{13}C NMR spectra (500 MHz and 125.7 MHz, $CDCl_3$) of **14**

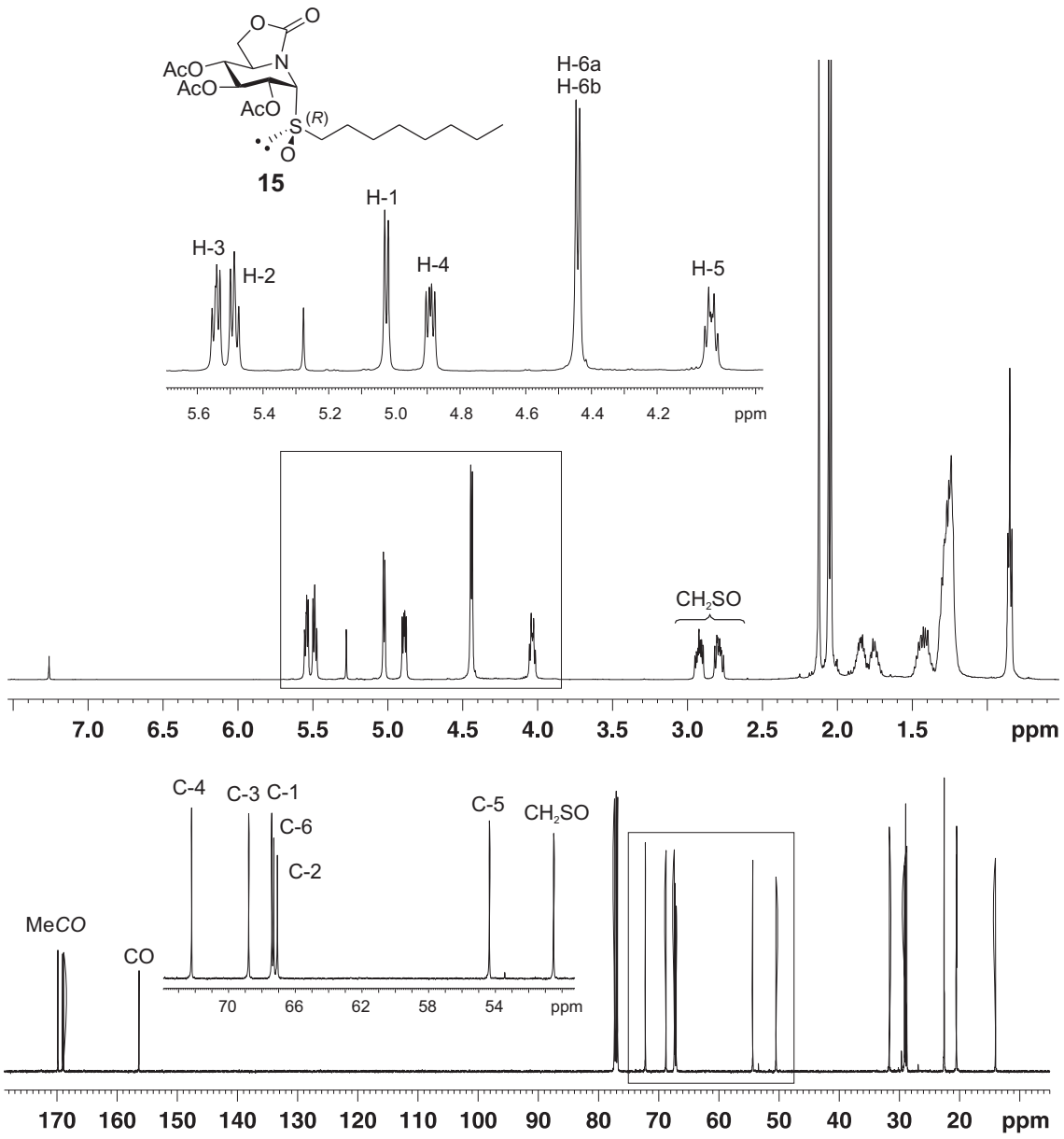

Figure S10. ^{1}H and ^{13}C NMR spectra (500 MHz and 125.7 MHz, $CDCl_3$) of **15**

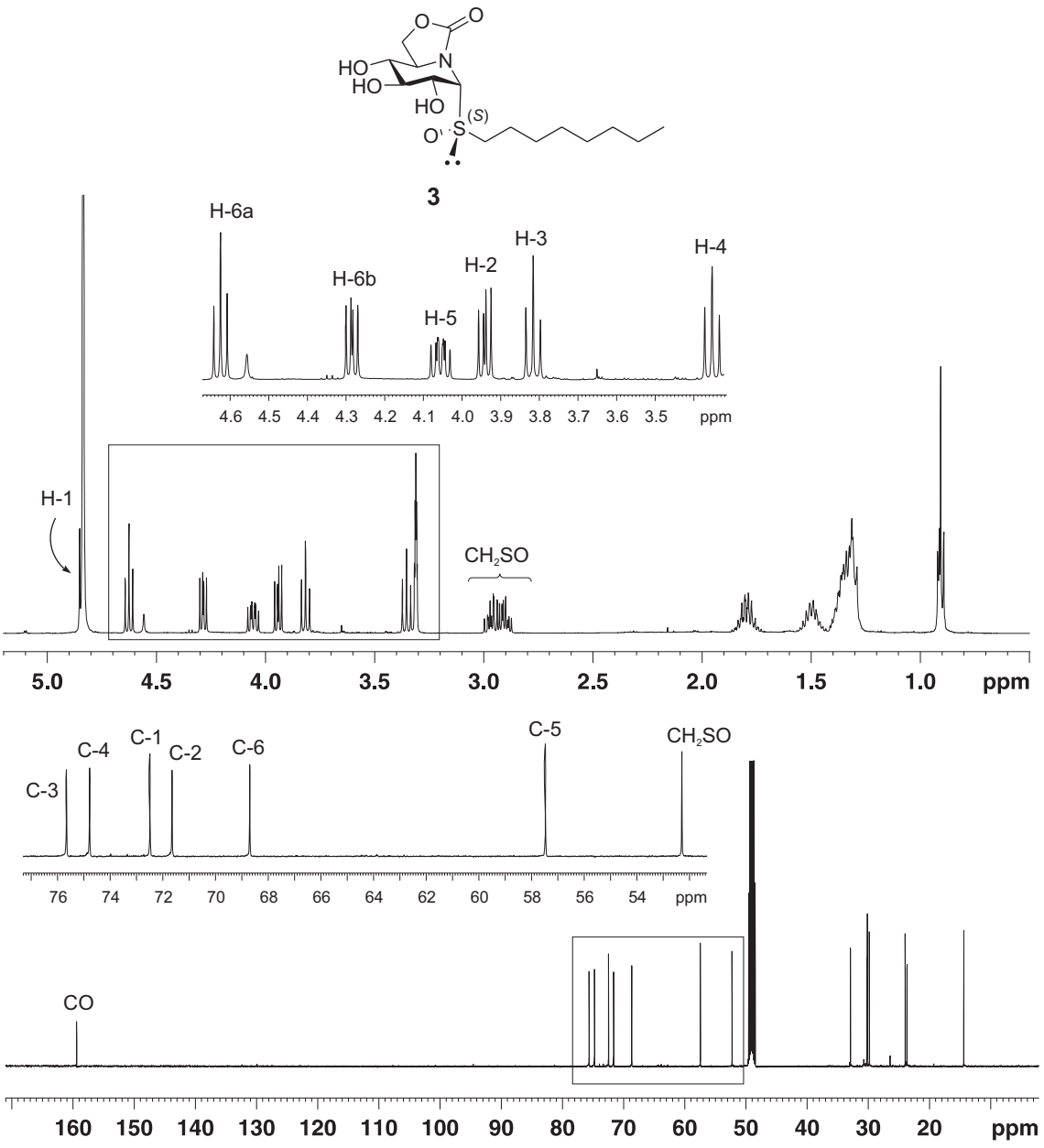

Figure S11. ^{1}H and ^{13}C NMR spectra (500 MHz and 125.7 MHz, CD_3OD) of **3**

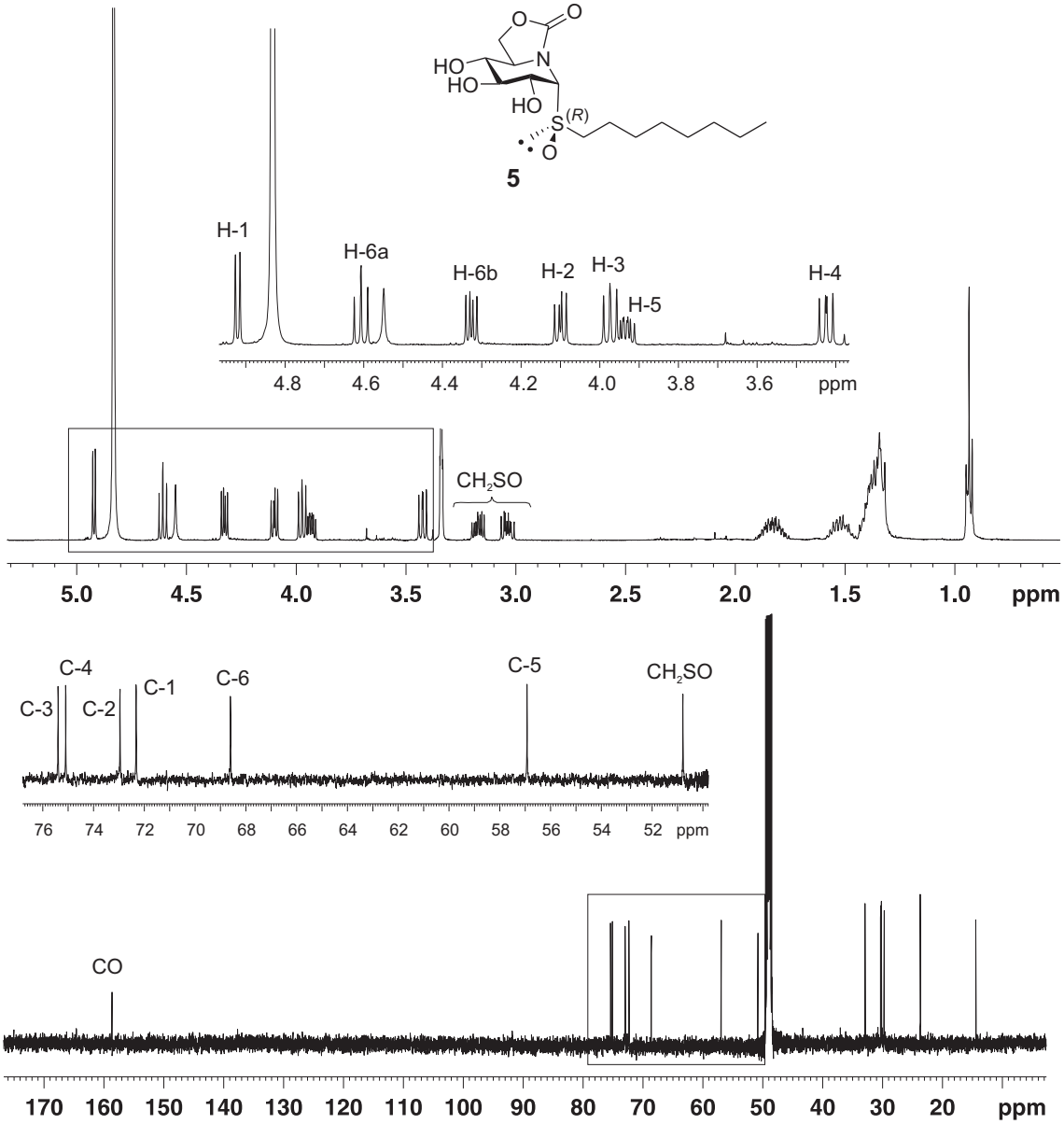

Figure S12. ^{1}H and ^{13}C NMR spectra (500 MHz and 125.7 MHz, CD_3OD) of **5**

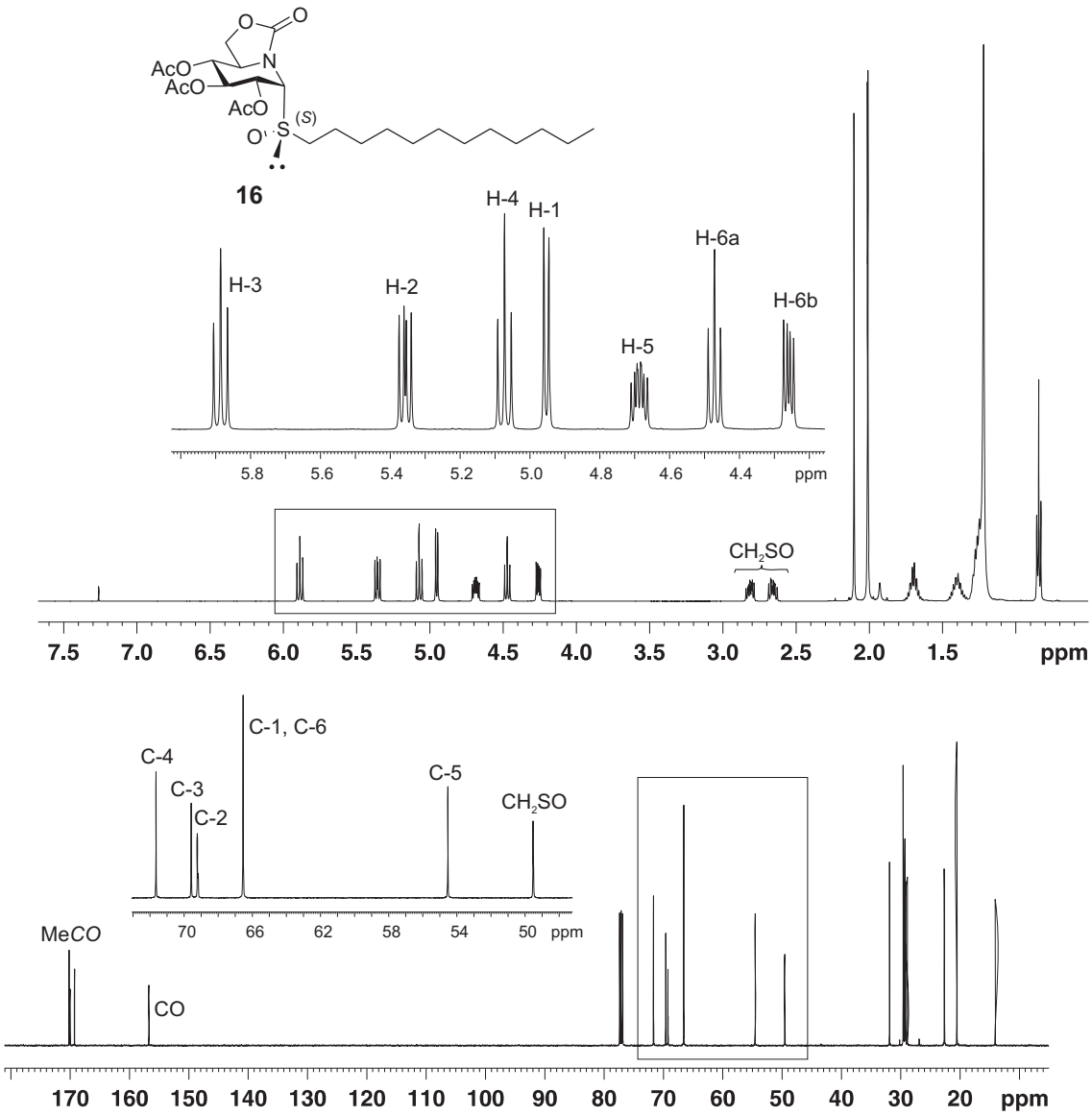

Figure S13. ^{1}H and ^{13}C NMR spectra (500 MHz and 125.7 MHz, $CDCl_3$) of **16**

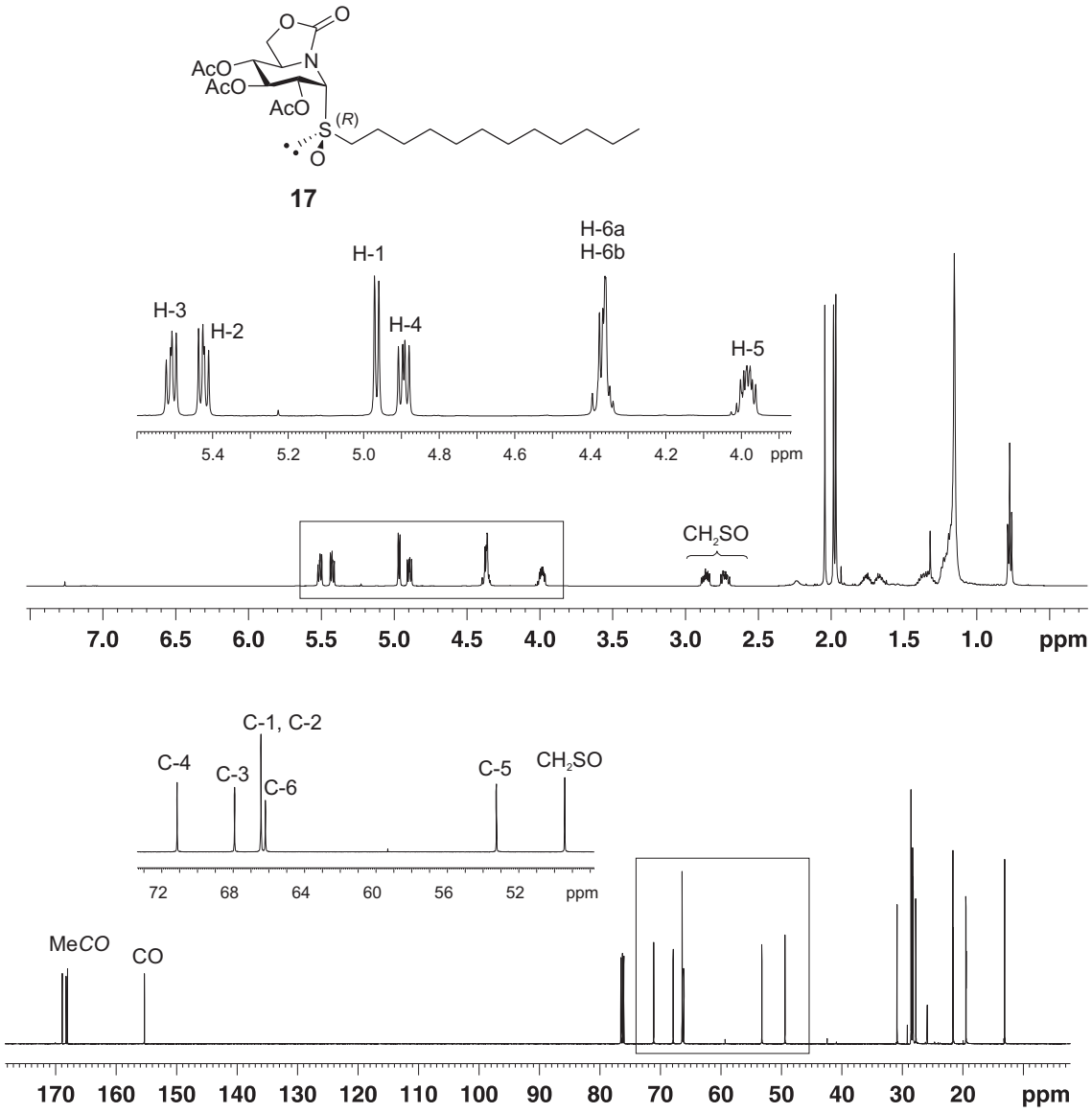

Figure S14. ^{1}H and ^{13}C NMR spectra (500 MHz and 125.7 MHz, $CDCl_3$) of **17**

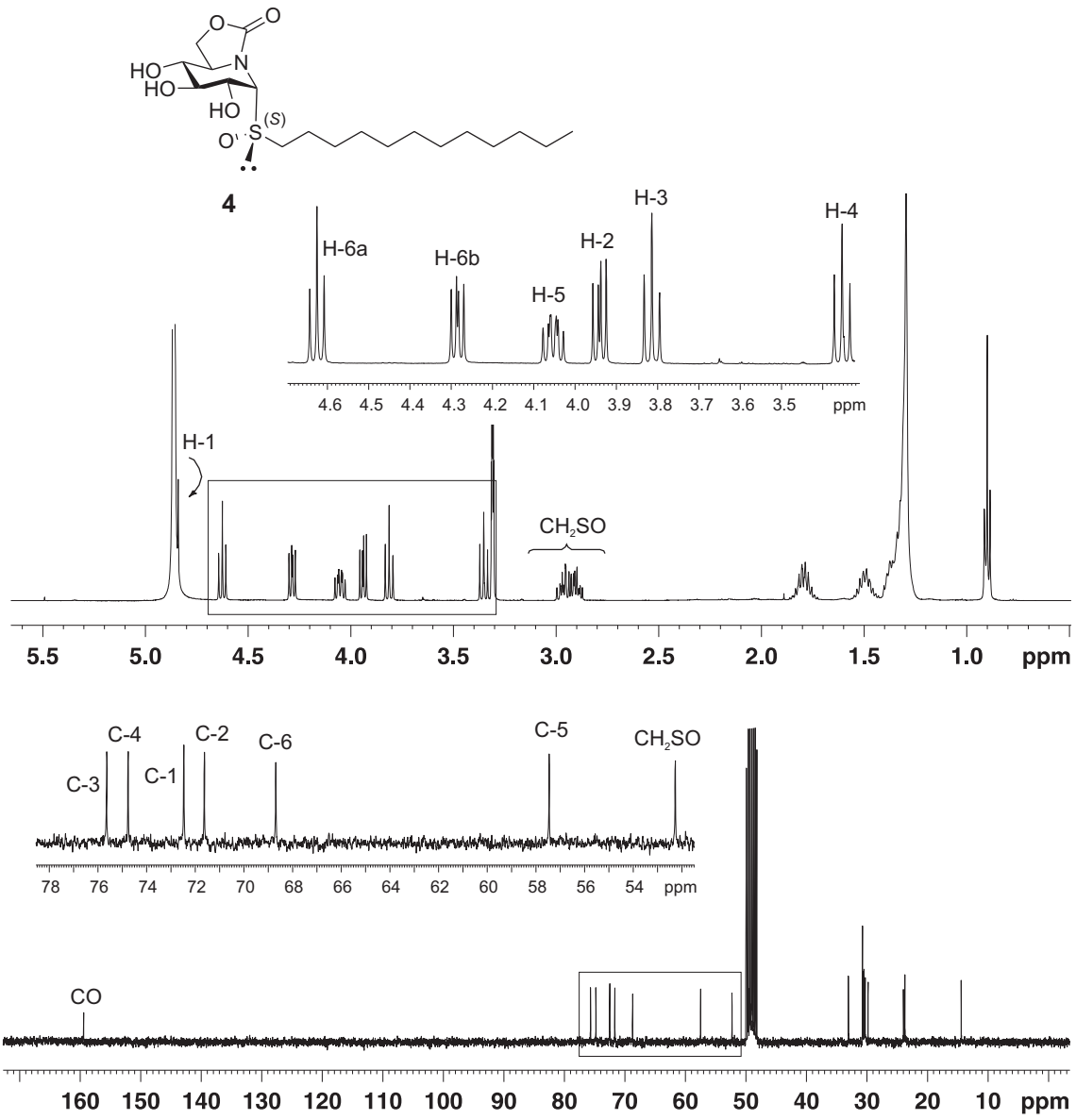

Figure S15. ^{1}H and ^{13}C NMR spectra (500 MHz and 75.5 MHz, CD_3OD) of **4**

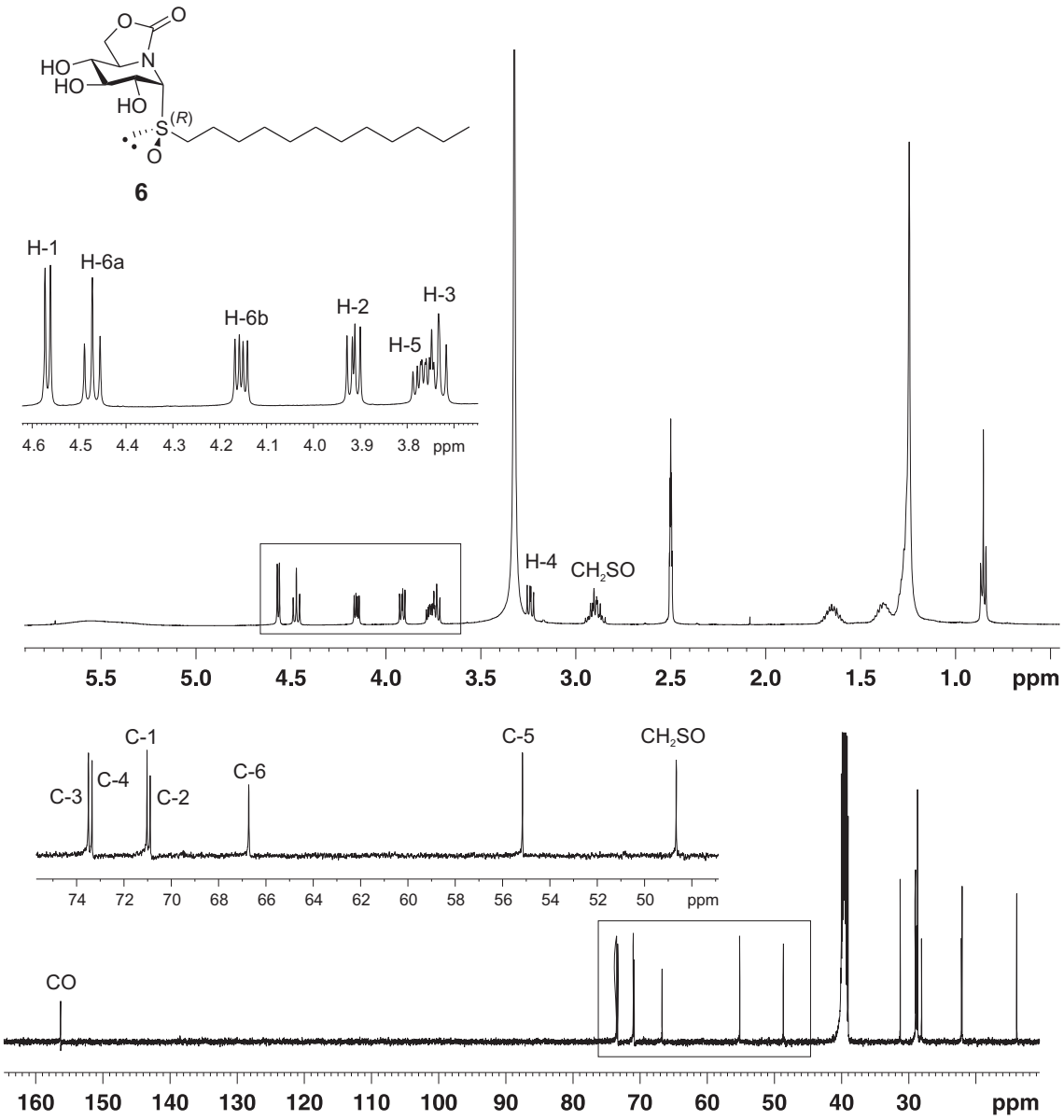

Figure S16. ^{1}H and ^{13}C NMR spectra (500 MHz and 125.7 MHz, DMSO-d_6) of **6**

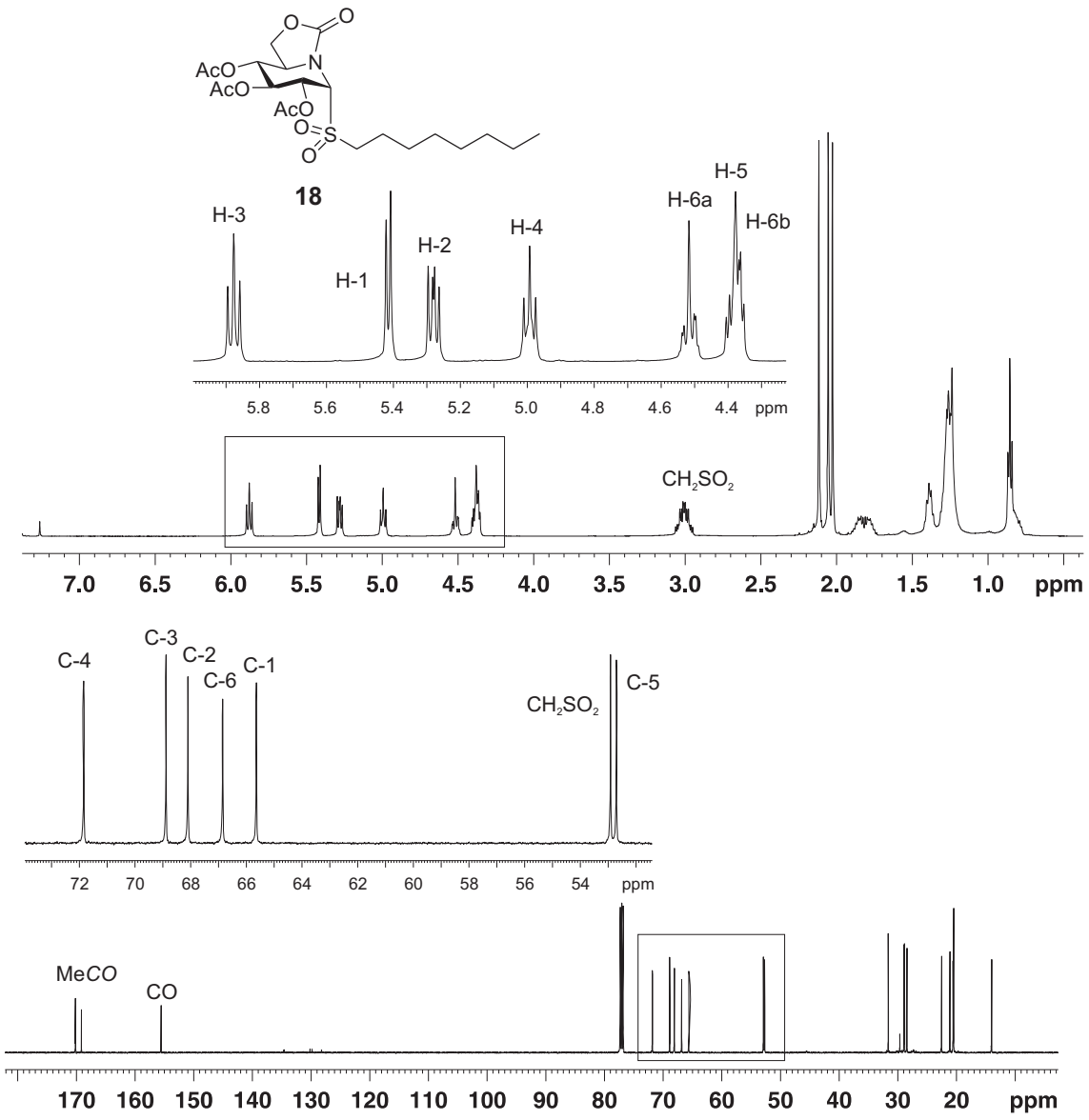

Figure S17. ^{1}H and ^{13}C NMR spectra (500 MHz and 125.7 MHz, $CDCl_3$) of **18**

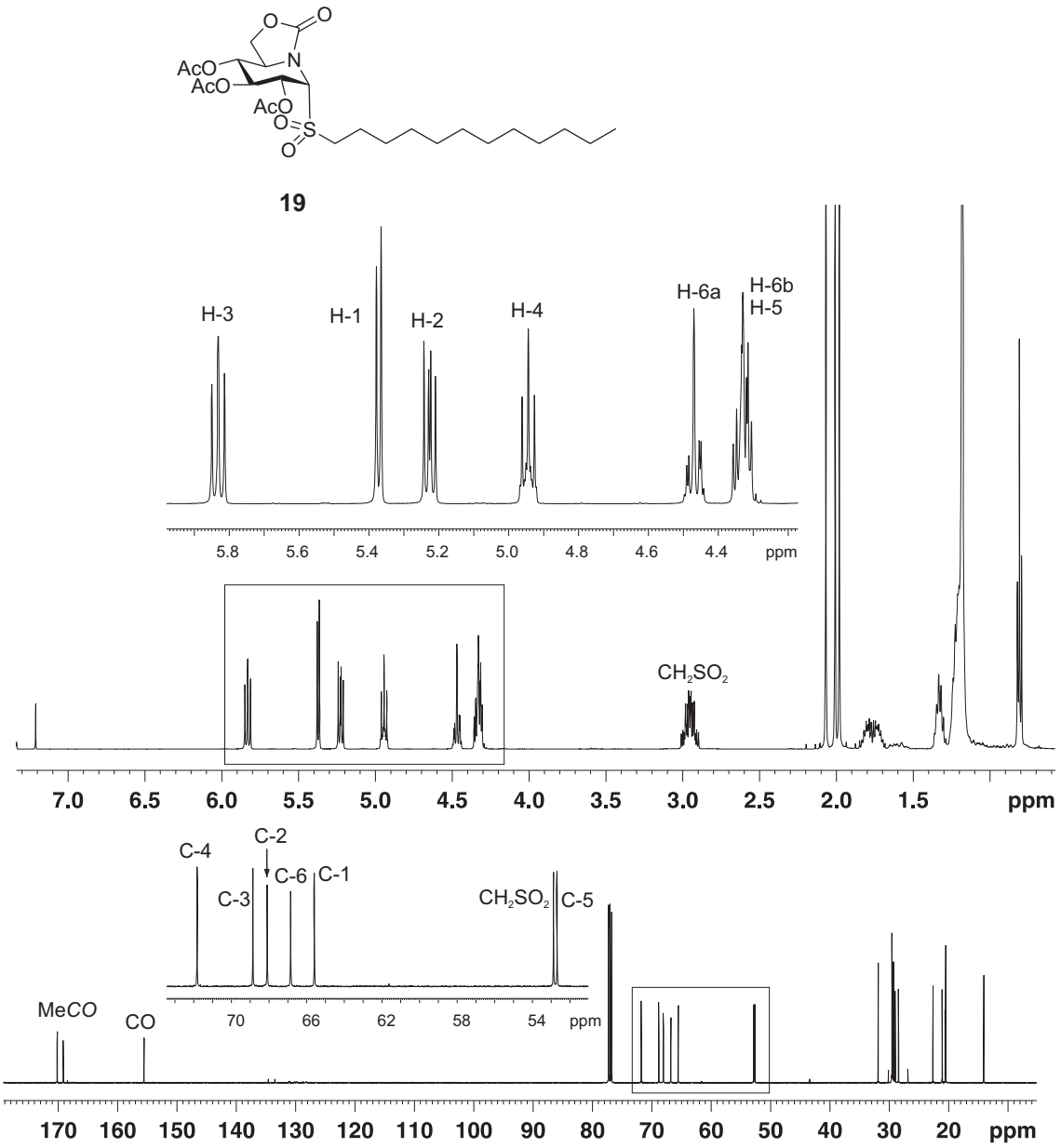

Figure S18. ^{1}H and ^{13}C NMR spectra (500 MHz and 125.7 MHz, $CDCl_3$) of **19**

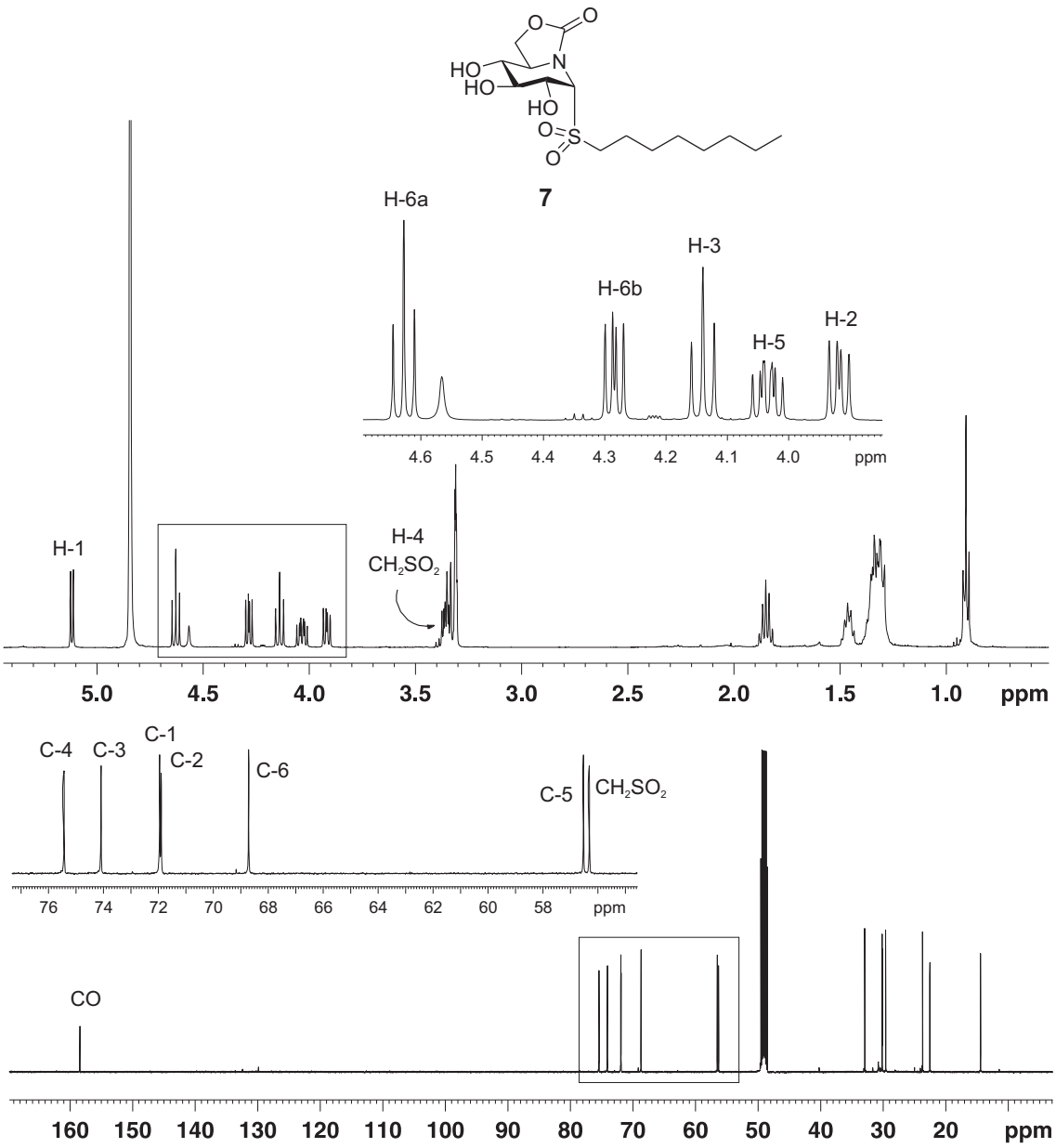

Figure S19. ^{1}H and ^{13}C NMR spectra (500 MHz and 125.7 MHz, CD_3OD) of **7**

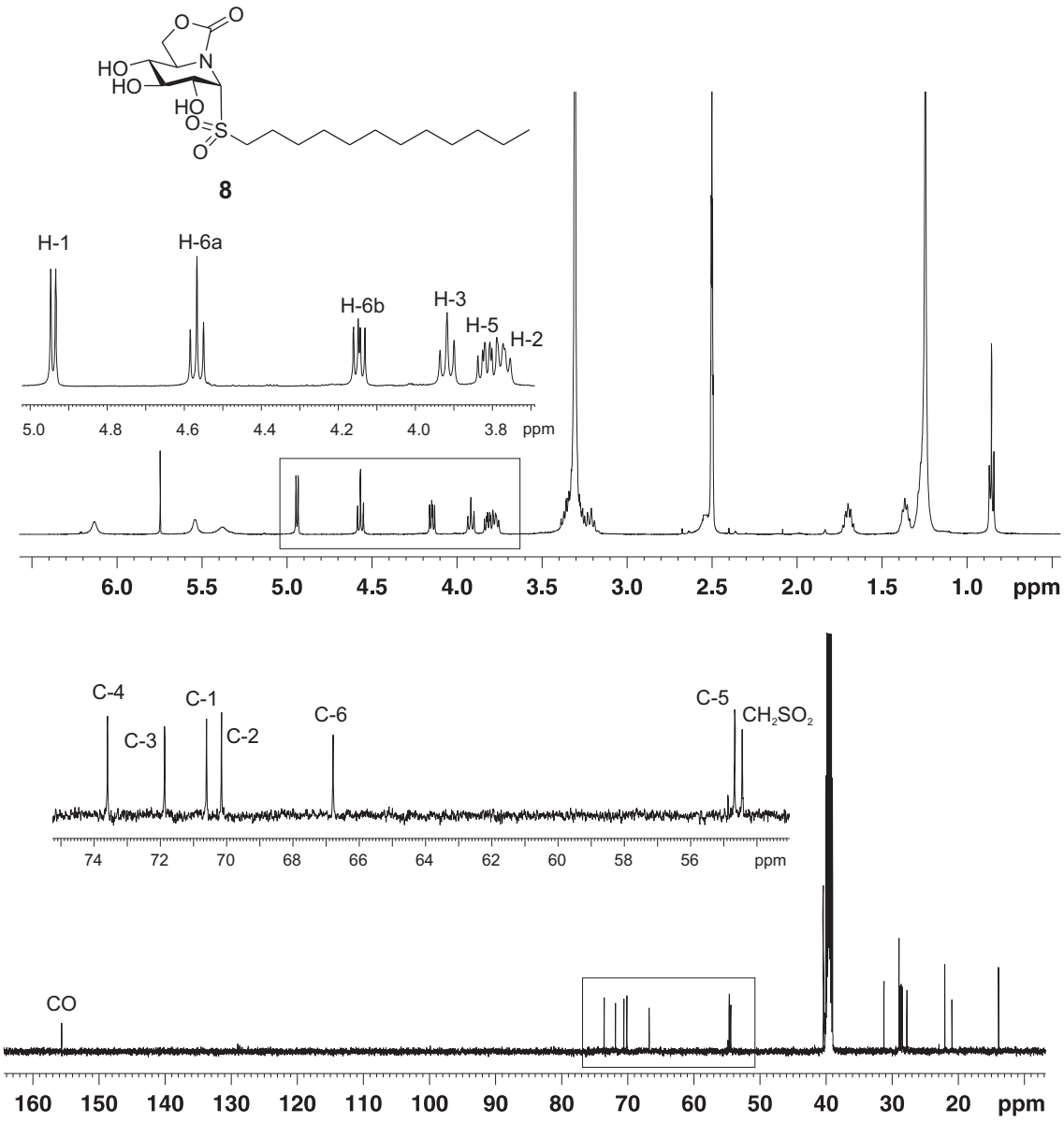

Figure S20. ^{1}H and ^{13}C NMR spectra (500 MHz and 125.7 MHz, DMSO-d_6) of **8**